Tubular permanent magnet actuators: cogging forces characterization

TUBULAR PERMANENT MAGNET ACTUATORS: COGGING FORCES CHARACTERIZATION

Johannes J.H. Paulides, *Member*, *IEEE,* Jeroen L.G. Janssen, *Student Member*, *IEEE,* Laurentiu Encica, *Member*, *IEEE* and Elena A. Lomonova, *Senior Member*, *IEEE*

Abstract: **Tubular permanent magnet actuators are evermore used in demanding industrial and automotive applications. However, these actuators can suffer from large cogging forces, which have a destabilizing effect on the servo control system and compromise position and speed control accuracy. This paper focuses on the identification of the cogging forces by means of finite element software, where an approach is introduced within the 2D finite element analysis to model the linear tubular permanent magnet actuator compared to conventional axisymmetrical models. This gives that the contribution of the stator teeth and finite length of the ferromagnetic armature core to the total cogging force can be separately analyzed. The cogging force predictions is characterized and the effectiveness of the new method is verified comparing the results of the tubular structure in both the axisymmetrical model and 2D finite element model, normally used for rotary machines.**

Index Terms**: cogging force, tubular actuator, linear, permanent magnet, cylindrical, brushless.**

I. INTRODUCTION

Linear direct-drive permanent magnet actuators are increasingly applied in industrial and automotive applications, because they can provide forces directly to a payload, i.e. in the absence of gearbox or transmission systems. They offer numerous advantages over rotary-to-linear-motion systems, with regard to their simplicity, efficiency, positioning accuracy and dynamic performance, in terms of their acceleration capability and bandwidth [1]. Comparisons of various linear actuator configurations showed that the tubular permanent magnet actuators (TPMA), as shown in Fig. 1, have the highest efficiency, offer a high power/force density, excellent servo characteristics, no end-windings, and, ideally, zero net attractive force between the stator and translator [2].

Although that the tubular actuator has numerous advantages, still the permanent magnets in the TPMA interact with the slotted armature structure and the finite-length stator core. The translator has a tendency to align in a position which corresponds to maximum magnetic energy, resulting in a cogging force. For many applications, the cogging force should be characterized and mitigated, however, ideally not at the cost of thrust force.

In flat linear and rotary permanent magnet machines numerous methods can be used to minimize the stator slotting cogging force, which are more or less also effective for the tubular structure. For example, permanent magnet length optimization, the use of semi-closed slots or magnetic slot wedges, skewing, varying the length of the air gap, permanent magnet shape optimization, etc. [3-5]. Also, fractional-slot-per-pole modular permanent-magnet-machine topologies can result in a negligible stator slotting cogging force [6]. Further, the end cogging force due to the finite armature length can be reduced by utilizing the counteracting nature of the force components on each end face of the armature core, which act in opposite directions [7]. Therefore, optimizing the armature or stator-core length ensures that the cogging-force components associated with both end faces can cancel each other. Also, shaping or smoothing the axial end corners also can significantly reduce the cogging due to the axial end-effects. However, for actuators that exhibit a relatively small effective airgap, hence increased power/force density, a significant end-effect cogging force could still exist.

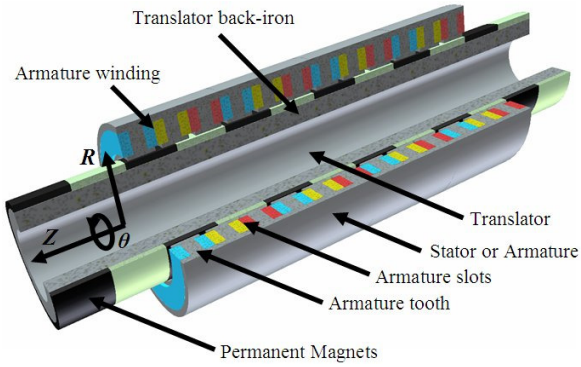

Fig.1 – Cross-section of the 3-phase slotted tubular brushless permanent magnet (PM) actuator.

Significant disadvantages of all linear and tubular machines are the end effects, caused by the interaction between the ends of the moving translator and the fixed armature. These effects play a significant role in the total cogging force of the device and should be minimized. However, when initially designing the tubular actuator, the focus is on minimizing the cogging due to interaction between stator teeth and translator magnets, and on producing maximum force within the set volume boundaries. A time efficient way to model the various cogging force components in linear machines is to use a single-sided flat rotary finite element model.

This paper proposes the use of such a 2D axial rotational finite element (FE) technique to represent the tubular axisymmetric translating model. This

technique is used to investigate both cogging components. However, although that the proposed technique can be applied both to tubular and linear topologies of permanent-magnet actuators, the effectiveness is confirmed by finite-element analysis on the tubular permanent magnet actuator structure. As such, Section II distinguishes various cogging force estimation techniques and Section III provides the results form the commonly used axisymmetrical finite element modelling technique. The newly proposed method is given in Section IV, where the total procedure is explained. This, however, does include the end-effects, which can be eliminated from the analysis as illustrated in Section V by a periodical 2D model which solely includes cogging due to the stator teeth. Section VI introduces a separate model, where the stator teeth are fully connected, that solely provides the end-effect component of the cogging force, which agrees well with the segregation method from section IV. Finally, Section VII presents the conclusions.

II. COGGING FORCE ESTIMATION

The fringing effect, associated with the finite length of the ferromagnetic armature core, produces cogging force. This causes the armature to align in a position that corresponds to maximum stored magnetic energy when unexcited. This component of cogging force results primarily from the normal forces, which are developed on each end face of the armature core. The two components are unidirectional and act in opposite directions. However, in slotted tubular permanent magnet actuators another cogging force component exist, which results from the interaction of the permanent magnet field with the permeance function of the slotted core.

A vast amount of research has been undertaken on the interaction of PMs with ferromagnetic or nonmagnetic slotted or slotless back-irons [3-11]. Commonly a finite-element analysis is used to investigate cogging in complex structures, for example, a tubular axially magnetized PM actuator with slotted pole pieces [8]. Additionally, also finite-element model are used to validate simple analytical techniques, e.g., to synthesize the cogging torque waveform which is associated with the stator slots [9].

However, in tubular actuators the slotting effect and its related cogging force are difficult to be determined in a straightforward way. Therefore, also Schwarz-Christoffel (SC) conformal mapping methods have been applied to the analysis of the tubular PM actuator. This mapping allows for field calculation in a domain where standard field solutions can be used, however assumes the iron to be infinitely permeable [10, 11]. The tubular structure of the machine gives some complications since the SC-mapping technique only applies to two-dimensional Cartesian domains. A mapping based upon 'unrolling' and 'stretching' the tubular machine into a linear machine is used to tackle this problem. Furthermore, the modelling of coils and magnets in the mapping domain is considered and the results are verified with finite element (FE) software of FLUX.

Although all the analytical and mapping methods are very elegant and fast, for a slotted geometry, the slotting effect is difficult to incorporate accurately. Especially in tubular permanent magnet actuators when thin tooth tips, complex tooth shapes, 3D armature end contours, thick laminations or even solid back-irons are used that give significant flux leakage, fringing effects or local magnetic saturation. Further, separation of the cogging forces in tubular machines is difficult and ultimately when skewing has to be investigated complex 3D finite element modeling is necessary [12].

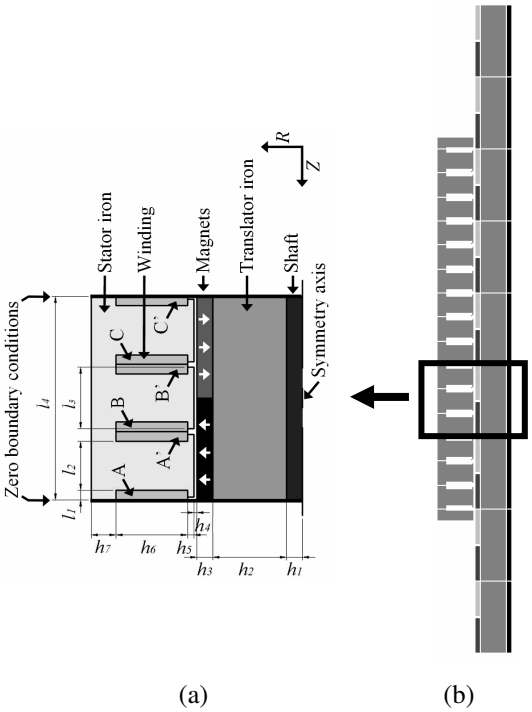

Fig.2 – Axisymmetrical view of the three phase brushless radially magnetized tubular permanent magnet actuator, where (a) shows topology and design variables (model A) and (b) shows the full geometry (model B).

III. AXISYMMETRICAL FINITE ELEMENT MODELING

The slotted tubular permanent magnet actuator under investigation has been previously optimized [13]. To optimize this actuator a space mapping optimization technique [14] is considered for deriving the actuator design, since it combines the advantages of the analytical determination of the machine performance (commonly used for design optimization and dynamic modeling) and finite element analysis (this is time demanding and inefficient for design optimization). Space mapping speeds up the design procedure by exploiting a combination of fast, less

accurate (coarse) models and time expensive, accurate (fine) models. The misalignment between the coarse and fine models is corrected by means of a mapping function, which is iteratively updated.

The algorithm used is detailed in [15], where the geometry of the 245(I) machine of [13] has been used, as shown in Fig. 2a, with the specific sizes summarized in Table 1. This design is obtained by an optimization method applied for a single pole-pair, and extended to five pole-pairs representing the complete tubular actuator, as shown in Fig. 2b. As shown in Fig. 2a this model uses the zero boundary conditions on the model edges.

Table 1. Actuator sizes in the axisymmetrical model

h_1 (mm)	5.0	h_7 *(mm)*	7.8
h_2 (mm)	23.3	l_1 *(mm)*	3.0
h_3 (mm)	5.0	l_2 *(mm)*	15.5
h_4 (mm)	1.0	l_3 *(mm)*	19.1
h_5 (mm)	2.0	l_4 *(mm)*	64.6
h_6 (mm)	22.5	l_{total} *(mm)*	323

The single pole-pair model, hereafter referred to as model A, assumes a current density of 15 A/mm^2, a coil packing factor of 0.5, mildsteel (AI1010 steel) and a NdFeB PM with a remanent flux density of 1.23 T and a recoil permeability of 1.1. Fig. 3 shows the used mesh, where the calculated static actuator force for model A, by finite element analysis, is respectively 242 N.

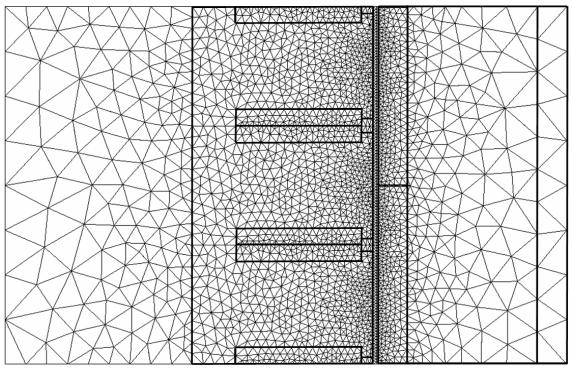

Fig.3 – Plot of the mesh density as used in the axisymmetrical models A and B.

Subsequently, the force is determined for the full-scaled axisymmetrical model of Fig. 2b, hereafter referred to as model B. The static force calculated for this model in the shown position is equal to 1446N, exceeding five times the force value of 242N, calculated for model A, due to the absence of zero flux boundaries between the pole-pairs.

These force amplitudes are valid for fixed position calculations, and hence neither magnetostatic nor transient position dependant force are taken into account. Such a magnetostatic force without considering a current, commonly referred to as a cogging or detent force, is calculated for model B (shown by Fig. 4), where the force, normalized to a movement equivalent to two pole pitches or 360º electrical degrees over the z-axis, is presented.

Fig. 4 clearly illustrates that for this axisymmetrical model the cogging force is rather high (approximately 10% of the rated force). This cogging force is a consequence of using PMs and can be separated into two parts: the first part is due to end effects on both sides of the stator of the tubular machine, and the second part is due to the slot openings in between the stator teeth. The separation of these parts is not applicable in conventional rotary machines, since no end-effects are apparent when modeling in 2D, and therefore all the cogging force is due to the slot openings. Conversely, for the linear actuator, as shown by Fig. 2b, the two parts can be split and investigated by applying periodic boundary conditions. Meanwhile, in axisymmetrical modeling these boundaries are not applicable, thus the separation of the cogging force components is not achievable for axisymmetrical models. Therefore, a distinctive 2D model representation is introduced in the next section, in which the linear actuator is represented as a rotary machine in order to distinguish the two cogging force components.

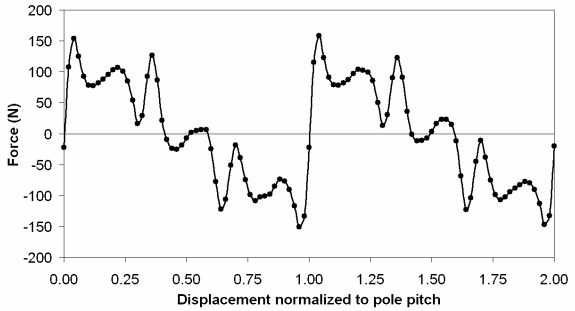

Fig.4 – Cogging force calculated for the axisymmetrical model B of the brushless tubular actuator.

IV. AXIAL 2D FINITE ELEMENT MODELING

In the proposed method, the tubular actuator is axially unfolded. Subsequently, this flat, single sided, linear machine is transformed into a rotary machine by rotating it around a central axis having a very large radius, which minimizes the curvature of the rotational 2D representation, as illustrated in Fig. 5. The axial length of this 2D model is equal to the airgap circumference of the tubular actuator.

The airgap radius is chosen such that for one pole-pair the non-linearity, the radial deviation, between air gap radius and its tangential, is less than 0.5 mm (measured between the end and middle of the stator inner bore). This corresponds to a pole-pair angle of 3.6 ° with an airgap radius of approximately 1 m, as

shown in Fig. 6. In case of the full-scale actuator this non-linearity is increased to 12.7 mm, model B of Fig. 2b. Further, the axial geometric parameters from the axisymmetrical model (model A) are linearly transformed into the angles in the 2D rotating model (model C), which, due to the small non-linearity discussed above, is a reasonable assumption.

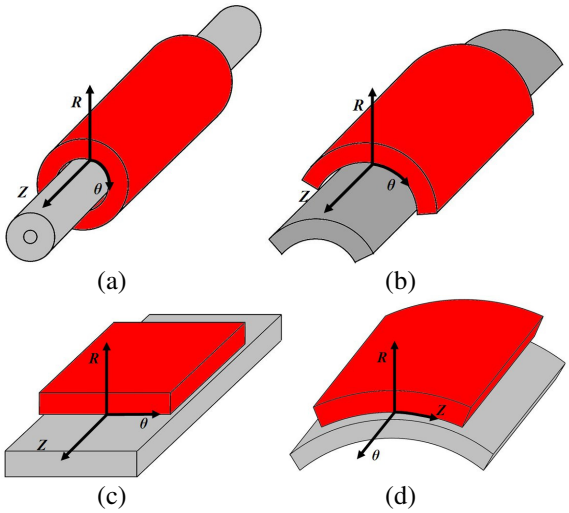

Fig.5 – Unrolling the axisymmetrical model to enable 2D rotational finite element model.

To compensate for the difference in the distance of the circumference as opposed to using a common axial length, introduced by representing the axisymmetrical model as a rotary machine, the radial sizes of the airgap, tooth tips, magnet and stator and rotor back iron are chosen in such a way that their respective volumes are equal to the volumes of these regions in the tubular model as shown in Table 2.

Table 2. Actuator sizes in the 2D rotating model

d_1 (mm)	5.0	d_7 (mm)	14.2
d_2 (mm)	11.8	β_1 (deg)	0.17
d_3 (mm)	4.6	β_2 (deg)	0.86
d_4 (mm)	1.0	β_3 (deg)	1.06
d_5 (mm)	2.1	β_4 (deg)	3.6
d_6 (mm)	22.5	R_{airgap} (mm)	1028

This ensures that the change in reluctance is kept at a minimum. However, in order not to impair on the tooth and winding geometry, the radial length of the stator teeth is not adjusted, which has the advantage that current density in the slots does not have to be altered in order to produce the same MMF and changes in slot leakage are minimized. A zero flux boundary condition is imposed on the inner bore of the rotor shaft, since this represents the symmetry axis in the axisymmetrical model, as shown in Fig. 2a and 7a.

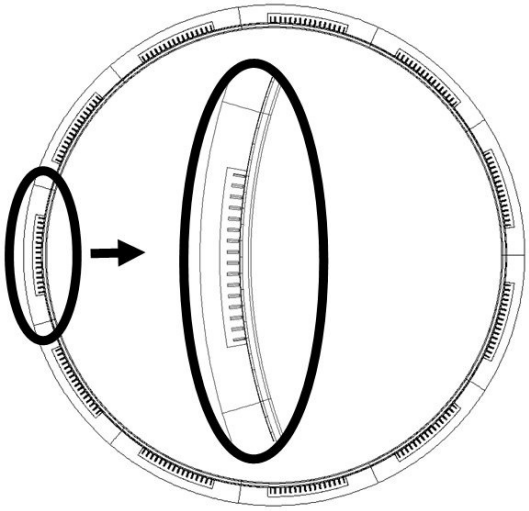

Fig.6 – 2D rotational model of the three phase brushless radially magnetized tubular permanent magnet actuator, where illustrating the full geometry and linear actuator.

The comparison, in terms of static force, between the axisymmetrical, model A, and the flat 2D representation, model C, is performed by the periodical model of Fig. 7a, albeit with zero flux boundaries. As Table 3 shows, the difference in produced force between A and this model, from now on referred to as C, is approximately 8%, due to the assumptions and concessions that have been made in the transformation from the axisymmetrical model to the 2D rotating model.

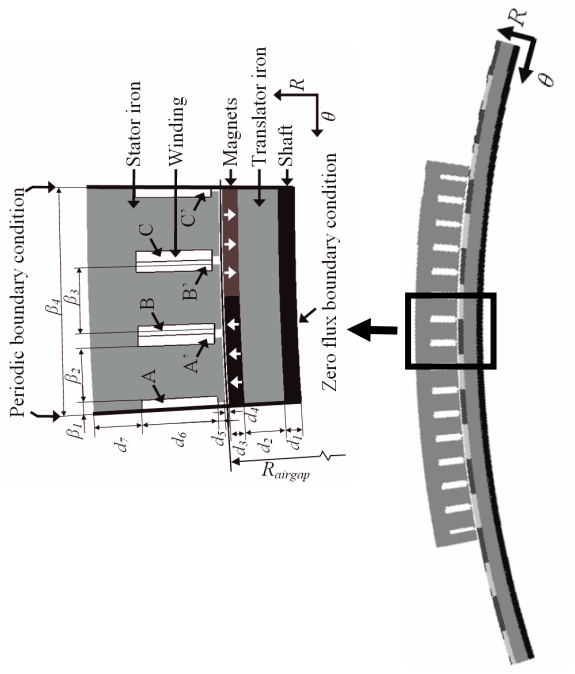

Fig.7 – 2D rotational view (R-θ) of the three phase brushless radially magnetized tubular permanent magnet actuator, where (a) shows topology and design variables (referred to as model C with zero boundary conditions and model E with periodic boundary conditions) and (b) shows the full geometry (model D).

Table 3. Calculated force for the models A to E

Model	Force	Figure	Model Boundary	Elements
(A)	242N	Fig. 2a	Zero	5140
(B)	1446N	Fig. 2b	Zero	30353
(C)	262N	Fig. 7a	Zero	4079
(D)	1528N	Fig. 7b	Zero	19261
(D)	300N	Fig. 7a	Periodic	4079

Having verified the magnetostatic equivalence between the model A and model C for the PM tubular actuator, a comparison on cogging forces is made for the full actuator geometry. A new model, referred to as model D and shown in Fig. 7b, is related to the rotating periodical model similar to the manner in which B is related to A in the translating geometry. It exhibits periodic boundary conditions on both rotor sides, thus no end effects due to the magnet array, which is a reasonable assumption since the stator ends remain at a certain distance from the rotor ends in the simulations. Furthermore, zero flux boundaries are applied at the sides of the stator area which includes large volume of air on both sides of the stator.

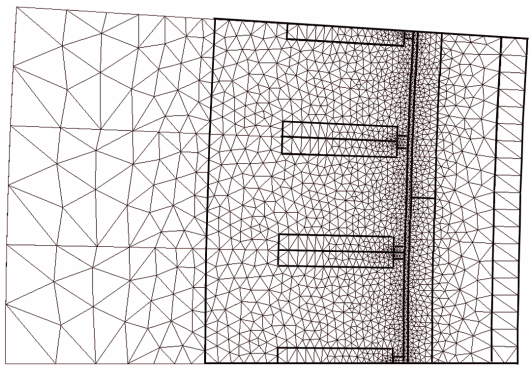

Fig.8 – Plot of the mesh density as used in the rotational 2D models C and D.

The calculated magnetostatic force is summarized in Table 3, which shows that the deviation between the two simulations is less than 6 %, respectively 1446 N (model B) and 1528 N (model D). The mesh density and mesh size, in each periodical part of the machine, are shown in Fig. 8 and Table 3, respectively.

Fig. 9 shows the resulting cogging force for models B and D, which demonstrates the similarity in force amplitude and shape for both topologies. This validates the use of the 2D rotating model (model D) as shown in Fig. 7b, to investigate the two separate parts of the cogging force for the three phase brushless radially magnetized tubular permanent magnet actuator.

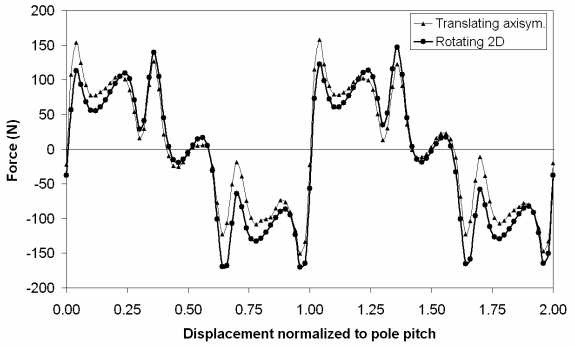

Fig.9 – Cogging force calculated for the axisymmetrical model B and for the 2D rotating model D of the brushless tubular actuator.

V. COGGING BEHAVIOR DUE TO THE STATOR TEETH

The partial representations, models A and C, as well as the full-model representations, models B and D, have demonstrated their respective similarities, as illustrated by Table 3 and Fig. 9. Therefore, the periodical model shown in Fig. 7a, model E, is used to obtain the cogging force due to the presence of the stator teeth part only, excluding the end effects. This representation assumes that the axial length of the actuator is infinitely long. The magnetostatic force amplitude simulation gives a static force of 300 N for this model, which closely approaches one-fifth of the force calculated for the full actuator, as summarized in Table 3. The resulting cogging force comparison for this model E is shown in Fig. 10.

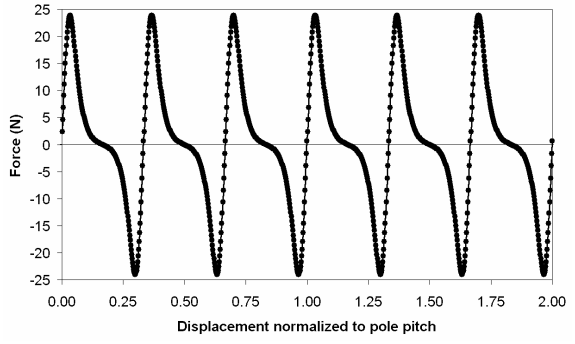

Fig.10 – Cogging force calculated for the rotational 2D model E which excludes end effects.

To obtain the cogging force due to stator teeth for the full actuator instead of one pole pair, the calculated force is multiplied by five, since the length of the actuator consists of five pole pairs. Both cogging characteristics are shown in Fig. 11, which demonstrates that the cogging force due to the stator teeth geometry has a strong influence on the total cogging behaviour of the actuator.

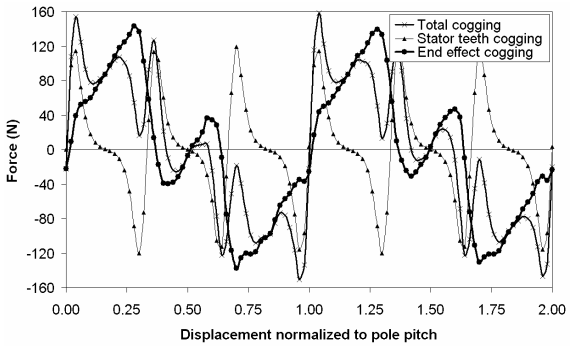

Fig.11 – Cogging force characteristics for model D (total cogging), the periodical model E (stator teeth cogging) and the difference of these two graphs (end effect part of the cogging force).

VI. COGGING BEHAVIOR DUE TO THE STATOR END EFFECTS

As demonstrated in the previous section, cogging force due to the stator teeth geometry is of significant influence on the total cogging behavior of the actuator, as shown in Fig. 11. This figure provides both the cogging characteristic for the full tubular actuator, including stator end effects and teeth geometry effects, and for the periodical model, including teeth geometry effects and excluding stator end-effects. Taking the difference between those characteristics gives the cogging behavior of the tubular actuator due to the end effects. Fig. 11 shows this end effect cogging, herewith demonstrating that the end effects are of significant influence on the total cogging behavior of the PM.

In order to verify this resulting cogging behavior, the axisymmetrical model B is modified into a new one referred to as F-model to represent a tubular actuator without stator teeth geometry effects. In this model the stator tooth tips are extended in such a way that the inner side of the stator, at the airgap, is represented by a large surface of mild steel without slot openings, as shown in Fig. 12.

Using model F, the cogging force characteristic of the tubular permanent magnet actuator which does not produce any cogging force due to the stator teeth geometry, is established. This is due to the smooth inner stator surface, which exhibits the change in permeability seen by the magnets and thus no preferable positions, causing cogging force, exist. The cogging due to the end effects, however, still is present and can thus be compared to the end effect induced cogging shown in Fig. 11. Both the cogging force calculated with the rotational representation, models D and E, and that with the axial 2D, model F, are shown in Fig. 13. This clearly shows the similarity between the two models.

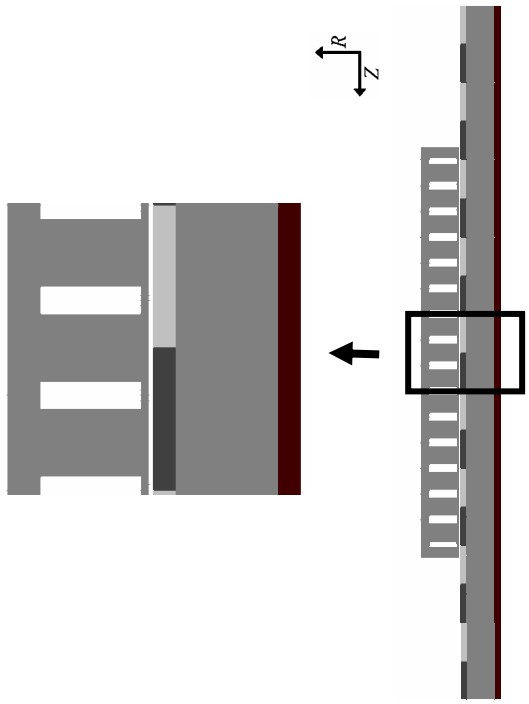

Fig.12 – Axisymmetrical view of the three phase brushless radially magnetized tubular permanent magnet actuator (model F) showing the full model and a magnification.

VII. CONCLUSION

The cogging forces both for contributions due to stator slotting and axial end-effects for the three-phase tubular PM actuator have been established. This has been achieved by comparing axisymmetrical models to single-sided flat rotary models to establish whether the 2D rotary representation is a suitable manner to model the tubular PM actuator geometry in FE analysis. From these models various ways to determine these two parts to the cogging force have been evaluated.

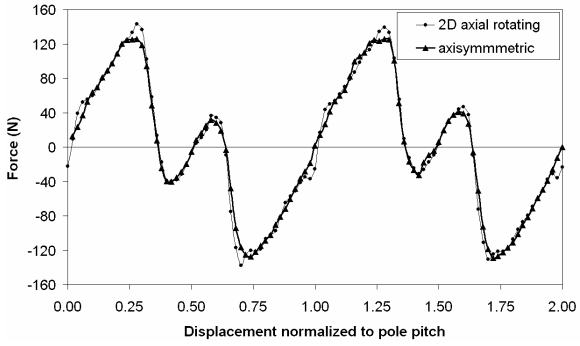

Fig.13 – End-effect induced cogging force for the axisymmetrical model obtained by model F and for the 2D axial rotating model obtained by the models D and E.

Finally, an axisymmetrical model without the influence of the stator teeth has been investigated, which verified the result of the 2D rotary FE analysis

method. It has been shown that the cogging due to the end-effects is similar to the stator teeth cogging, for this specific design, by respectively 140N and 120N. However, it should be mentioned that reducing the magnet pole pitch, generally to 0.7, will significantly reduce the cogging due to the stator teeth, albeit at some reduction in force density. Further, smoothing the axial end corners also significantly reduces the cogging due to the axial end-effects.

REFERENCES

[1]. M. Platen and G. Henneberger, 'Examination of leakage and end effects in a linear synchronous motor for vertical transportation by means of finite element computation', IEEE Transactions on Magnetics, Volume 37, No. 5, (2001) pp. 3640-3643.

[2]. I. Boldea, S.A. Nasar, "Linear electric actuators and generators", Cambridge University Press, (1997).

[3]. T. Li, and G. Slemon, 'Reduction of cogging torque in permanent magnet motors', IEEE Transactions on Magnetics, Volume 24, No. 6, (1988) pp. 2901-2903.

[4]. C. Breton, J. Bartolome, J.A Benito, G. Tassinario, I. Flotats, C.W. Lu, and B.J. Chalmers, 'Influence of machine symmetry on reduction of cogging torque in permanent-magnet brushless motors', IEEE Trans. on Magnetics, Volume 36, No. 5, (2000) pp. 3819-3823.

[5]. C.S. Koh, and J.S. Seol, 'New cogging-torque reduction method for brushless permanent-magnet motors', IEEE Transactions on Magnetics, Volume 39, No. 6, (2003) pp. 3503-3506,.

[6]. M. Inoue, J. Wang, and D. Howe, "Influence of slot openings in tubular modular permanent magnet machines", PROC. LDIA'2003, (2003) pp. 383–386.

[7]. J. Wang, M. Inoue, Y. Amara and D. Howe, 'Cogging-force-reduction techniques for linear permanent-magnet machines', IEE Proc.-Electr. Power Appl., Volume 152, No. 3, (2005) pp. 732-738.

[8]. M. Ashabani, J. Milimonfared, J. Shokrollahi-Moghani, S. Taghipour, M. Aghashabani, "Mitigation of Cogging Force in Axially Magnetized Tubular Permanent-Magnet Machines Using Iron Pole-Piece Slotting", IEEE Trans. on Magnetics, Volume 44, (2008) pp. 2158-2162.

[9]. Z.Q. Zhu, S. Ruangsinchaiwanich, D. Ishak, D. Howe, "Analysis of cogging torque in brushless Machines having nonuniformly distributed stator slots and stepped rotor magnets", IEEE Trans. on Magnetics, Volume 41, (2005) pp. 3910 – 3912.

[10]. B.L.J. Gysen, E.A. Lomonova, J.J.H. Paulides, A.J.A. Vandeput, "Analytical and Numerical Techniques for Solving Laplace and Poisson Equations in a Tubular Permanent Magnet Actuator: Part I. Semi-Analytical Framework, IEEE Trans. on Magnetics, Volume 44, (2008) pp. 1761-1767.

[11]. B.L.J. Gysen, E.A. Lomonova, J.J.H. Paulides, A.J.A. Vandeput, "Analytical and Numerical Techniques for Solving Laplace and Poisson Equations in a Tubular Permanent Magnet Actuator: Part II. Schwarz–Christoffel Mapping, IEEE Trans. on Magnetics, Volume 44, (2008) pp. 1761-1767.

[12]. J.L.G. Janssen, J.J.H. Paulides, E.A. Lomonova, A.J.A. Vandenput, "Cogging Force Reduction in Tubular Permanent Magnet Actuators", Electric Machines & Drives Conf. IEMDC '07, Volume 1, (2007) pp. 226-271.

[13]. J.J.H Paulides, L. Encica, E.A. Lomonova, A.J.A. Vandenput, "Design considerations for a semi-active electro-magnetic suspension system", IEEE Trans. On Magnetics, Volume 42, Issue 10, (2006) pp. 3446-3448.

[14]. J. W. Bandler, Q. S. Cheng, S. A. Dakroury, A. S. Mohamed, M. H. Bakr, K. Madsen, and J. Sondergaard, "Space mapping: the state of the art", IEEE Trans. Microwave Theory Tech., Volume 52, (2004) pp. 337-361.

[15]. L. Encica, D. Echeverría, E. A. Lomonova A. J. A. Vandenput, P. W. Hemker, L. Lahaye: "Efficient Optimal Design of Electromagnetic Actuators Using Space-Mapping", Structural and Multidisciplinary Optimization, Volume 33, No. 6, (2007) pp. 481-491.

1

---

[1] Johannes Paulides (j.j.h.paulides@tue.nl) was born in Waalwijk, The Netherlands in 1976. He received the B.Eng. degree from the Technische Hogeschool 's-Hertogenbosch in 1998 and the M.Phil. and Ph.D. degrees in electrical and electronical engineering from the University of Sheffield in 2000 and 2005, respectively. Since 2005, he has been a Research Associate at Eindhoven University of Technology, and simultaneously is a director of Paulides BV and Advanced Electromagnetics BV, small SMEs based in the Netherlands producing electrical machines and prototype electromagnetic devices. His research activities span all facets of electrical machines, however in particular linear and rotating permanent magnet excited machines for automotive and high precision applications.

Jeroen L.G. Janssen (j.l.g.janssen@tue.nl) was born in Boxmeer, The Netherlands in 1982. He received his B.Sc. and M.Sc. degree in Electrical Engineering at Eindhoven University of Technology, The Netherlands. Currently, he is pursuing a PhD degree within the Electromechanics and Power Electronics group at the same university. His research is focused on permanent-magnet based vibration isolation for lithographic applications.

Laurentiu Encica (l.encica@tue.nl) was born in Bucharest, Romania, in 1978. He received the Dipl. Eng. degree from the University "Politehnica" of Bucharest, Romania, in 2002, and the Ph.D. degree from the Eindhoven University of Technology, Eindhoven, The Netherlands, in 2008. He is currently affiliated as a post-doctoral researcher with the Eindhoven University of Technology, The Netherlands. His research interests are in computer assisted analysis, design and optimization of electromagnetic actuators.

Elena A. Lomonova (e.lomonova@tue.nl) was born in Moscow, Russia. She received the M.Sc. (cum laude) and Ph.D. (cum laude) degrees in electromechanical engineering from Moscow State Aviation Institute (TU), Moscow, Russia, in 1982 and 1993, respectively. She is currently an Associate Professor at Eindhoven University of Technology, Eindhoven, The Netherlands. She has worked on electromechanical actuators design, optimization, and development of advanced mechatronics systems.